Optimization of Shapes for Round Wire, High Frequency Gapped Inductor Windings

Jiankun Hu
C. R. Sullivan

Found in *IEEE Industry Applications Society Annual Meeting,* Oct. 1998, pp. 907–911.

IEEE Industry Applications Society
Annual Meeting
St. Louis, MO, 12-16 October, 1998

Optimization of Shapes for Round-Wire High-Frequency Gapped-Inductor Windings

Jiankun Hu Charles R. Sullivan
Thayer School of Engineering, Dartmouth College, Hanover, NH 03755, USA
Phone: (603)643-2851 Fax: (603)643-3856 E-Mail: chrs@dartmouth.edu
URL: http://thayer.dartmouth.edu/inductor

Abstract

A numerical method is used to determine the winding shape that minimizes total winding losses in a gapped inductor with round-wire windings. The algorithm accounts for proximity-effect loss that results from the two-dimensional field in the winding area, and for the effect of the winding on that field. Results are presented for an example geometry. The optimized configuration has significantly lower losses than alternative designs including lumped-gap and distributed-gap inductors with windings designed using standard one-dimensional analysis.

I. Introduction

In an inductor winding, the core, and particularly the air gap, strongly affect the field in the winding area, and thus determine proximity-effect losses. Conventional one-dimensional analyses of proximity-effect losses and the associated design methodologies developed for transformers [1], [2], [3], [4], [5], [6], [7], [8], [9], [10] do not account for the true field of a gapped inductor, and do not allow accurate prediction of inductor ac resistance [11]. This limitation is particularly important because of the growing popularity of soft-switching power-converter topologies, which require inductors with high ac current. Low ac resistance is essential for efficient operation.

One approach to this problem is to modify the core and gap to achieve a one-dimensional field configuration, for example by using a distributed gap as shown in Fig. 1 [12], [13]. Then standard one-dimensional winding design and analysis methods can be used. This solution is often motivated by avoiding the "fringing field" associated with the gap, which can impinge on the winding and increase losses. The quasi-distributed gap technique can be used to approximate a distributed gap without requiring a low-permeability material [14], [15], [16], [17], [18], [19], [20].

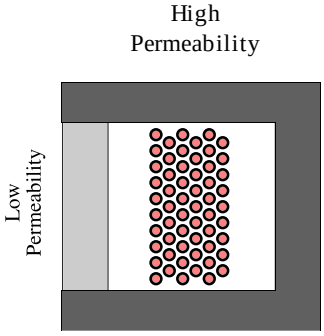

Fig. 1. Distributed-gap inductor design.

In this paper, we study an alternative approach: developing winding designs to minimize loss with a given gapped core structure, as explored in [21], [22]. We develop analysis of proximity-effect losses with the actual field distribution of a gapped inductor, and systematic optimization of the winding configuration to minimize losses. We consider two-dimensional analysis of round-wire windings including litz and single-strand wire; the fundamental approach could also be extended to three-dimensional analysis. Our original motivation was to find the lowest loss possible with the constraint of a single lumped gap, because this is less costly than a distributed or quasi-distributed gap. In fact, we found that the performance of the optimized lumped-gap design is, in many cases, even better than that of the corresponding distributed-gap design.

II. Analysis of Proximity-effect Losses

Direct numerical computation of eddy-current losses in wire windings with many turns or many strands is usually impractical, despite the availability of commercial finite-element analysis tools with the capability of analyzing eddy currents. This is because the mesh resolution required to model the individual strands is prohibitive. A much more computationally efficient approach uses the fact that proximity-effect losses are proportional to the square of the ac field impinging on any given conductor. This field may be accurately estimated by magnetostatic analysis, since eddy currents circulating within a small conductor cannot significantly perturb the overall field.

For cylindrical conductors with diameter, *d*, small compared to a skin depth, the proximity-effect loss in an ac field, *B*, perpendicular to the axis of the wire, at a frequency ω is [23],

$$P_{pe} = \frac{\pi \cdot \omega \cdot |\boldsymbol{B}|^2 \cdot l \cdot d^4}{128 \cdot \rho_c}, \qquad (1)$$

where *l* is the length of the conductor and ρ_c is the resistivity of the conductor. (For calculations for larger conductors, see [9].) From magnetostatic analysis, one can calculate the average value of the square of the flux density over the region of winding, $\overline{|B|^2}$, and then use this with (1) to calculate total

proximity-effect loss. This approach can be used with standard magnetostatic finite-element analysis or with other numerical or analytical methods of calculating the magnetostatic field. One derivation of the standard one-dimensional analysis uses this approach [23]. Reference [23] also describes an experimental measurement approach to obtain information equivalent to $\overline{|B|^2}$, which can then be used to predict losses.

III. Computation of Optimal Shape

Given a gapped inductor core, as shown in Fig. 2, we wish to find the winding configuration that provides minimum total loss for a given number of turns. Since solid-wire windings can be considered a special case of litz-wire windings with the number of strands equal to one, and because litz wire is particularly common and useful in inductors with high ac current, we consider litz-wire windings. One may optimize a litz-wire winding with or without constraints on cost-related parameters such as diameter of strands and number of strands [24]. We begin by optimizing the design with the strand diameter fixed, assumed to be constrained by cost or manufacturing considerations. The optimization problem becomes the choice of the number of strands in the litz bundle (assumed equal for each turn), and the positioning of the resulting bundles within the window. We solve the continuous approximation to this discrete problem: the number of strands is not limited to integers, and rather than finding the individual position for each turn, we find a region of the winding window, with area equal to the area of the wire (adjusted by a packing factor) that gives minimum total loss. The considerations involved include the tradeoff between lower ac loss with less copper and lower dc resistance with more copper; the positioning of the wire in regions of low field to minimize proximity-effect loss; and the effect of that position, in turn, on the field in the window area.

Our optimization program, COOS (Computation of Optimal Shape), divides the window into a grid of typically

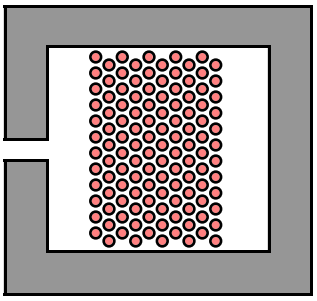

Fig. 2. Two-dimensional inductor configuration analyzed, shown with a winding that has not been optimized.

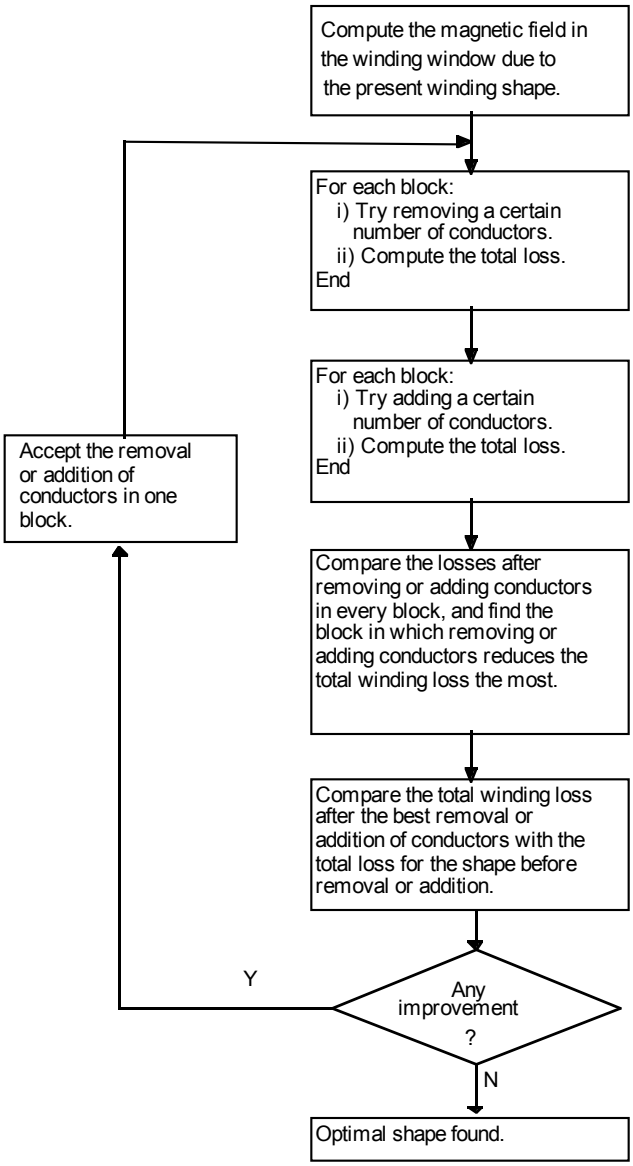

Fig. 3. Flow chart of the COOS optimization algorithm.

four hundred elements. The shape of the winding is represented by a matrix, $\mathbf{P}$, in which each element indicates whether that region is filled with wire ($\mathbf{P}(i,j) = 1$) or is empty ($\mathbf{P}(i,j) = 0$). Values between zero and one are also allowed, and indicate either sparse filling of a region, or a border between filled and empty regions that falls somewhere in the middle of the element. In practice, we found no sparsely filled regions in our solutions, but we did not wish to preclude that possibility prematurely.

The optimization problem is then to minimize the loss by adjusting the elements of $\mathbf{P}$, subject to the constraint of $0 \le \mathbf{P}(i,j) \le 1$. In principle, any multivariable optimization algorithm can be applied. We had good results using the procedure outlined in Fig. 3. Although this algorithm does

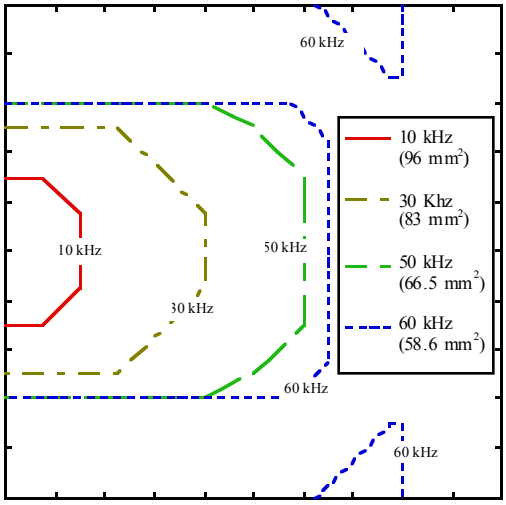

Fig. 4. Optimal winding shapes computed by COOS for a 10 mm x 10 mm winding window with a gap at the center left and 0.1 mm litz-wire strand diameter, for four frequencies. The area near the gap, bordered by the appropriate line for a given frequency, is empty of conductors. Cross-sectional area used by each solution is indicated. For the 60 kHz (58.6 mm^2) solution, additional empty areas appear at the top and bottom right.

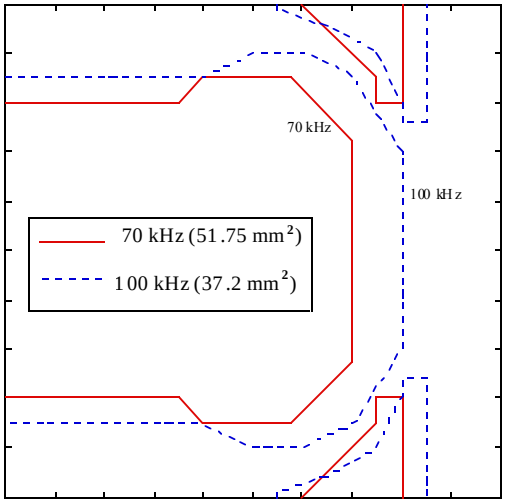

Fig. 5. Optimal winding shapes computed by COOS as in Fig. 4, but for higher frequencies. Areas empty of wire are bordered by the lines shown and include a "mushroom" shape based at the gap, bordered by the indicated line, and the wedges at the top and bottom right.

not guarantee finding a global minimum in loss, we found it converged to the same solution regardless of the initial configuration. The algorithm used a specialized approach to numerical computation of the field to take advantage of the structure of the problem, as described in the Appendix.

IV. Results

For a square winding window, 10 mm x 10 mm, and 0.1 mm strand diameter (approximately 38 AWG), we found optimal shapes for a range of frequencies, as shown in Figs. 4, 5 and 6. We used a 1 mm gap for most runs, but found that, consistent with [20], for small gaps, gap length does not significantly affect the results.

As the frequency increases and eddy currents become a more severe problem, the optimal solution includes a progressively larger "hollow" near the gap (Fig. 4). At still higher frequencies, this hollow takes on a slightly mushroomed shape and additional hollows appear near the corners (Fig. 5). Eventually, the winding areas on each side separate, and become thin layers on each of three sides (Fig. 6). The accuracy of the solutions is limited by the resolution of the grid breaking up the window into elements of the "shape matrix" **P**. Some details of the shapes shown are based on our judgment in interpreting the matrix.

A comparison of the proximity-effect loss results indicates the usefulness of the optimized shapes. It is not immediately clear what to compare our results to, as we do not believe there exists a standard design methodology for inductor design considering proximity-effect losses. Designs optimized on the basis of one-dimensional analysis are one possibility. We developed such designs and calculated actual loss using finite-element magnetostatic analysis as described in Section II, assuming that the winding is spaced away from the gap by a distance of twice the gap length (2 mm) as might occur with a typical bobbin and a center-post gap. Two-dimensional analysis of the designs based on one-

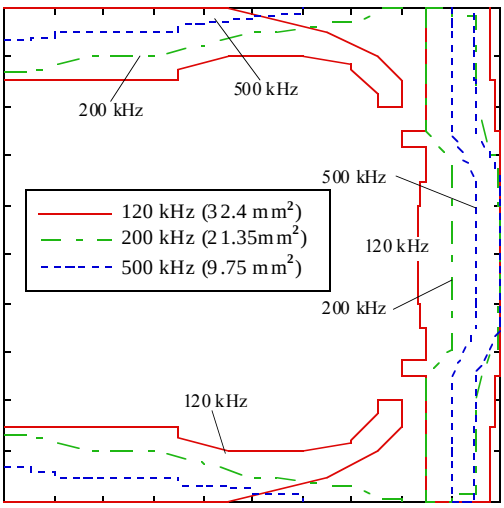

Fig. 6. Optimal winding shapes computed by COOS as in Figs. 4 and 5, but for higher frequencies. Conductors fill the indicated areas along the top and bottom walls and near the right wall.

dimensional analysis shows that they have substantially higher losses than the one-dimensional analysis predicts. But the optimized solution computed by COOS shows a dramatic improvement even over the overly optimistic one-dimensional prediction for the one-dimensional design (Fig. 7).

Comparisons with designs based on one-dimensional analysis clearly shows the value of the two dimensional analysis used in COOS. But this doesn't directly demonstrate the value of the unusual shapes developed by COOS. To asses the importance of the particular shapes, we compare their performance to that of a rectangular winding, chosen using two-dimensional analysis to minimize losses. The rectangular winding is then placed as far from the gap as possible, and the area is chosen to minimize losses. To give an overview of the performance of such solutions, and compare them to the optimal shape, we can plot $\overline{|B|^2}$ (a measure of proximity-effect losses) vs. the winding area used, A (an indicator of dc loss) (Fig. 8). Thus, we get a complete view of the design space spanned by the set of COOS-computed optimal shapes, and the corresponding possibilities with rectangular shapes. The COOS solutions consistently show a substantial advantage in ac loss for any given winding area, often by a factor of two or better.

Finally, we may compare this solution to the distributed-gap solution (Fig. 1), which has been considered ideal, by adding to the plot the value of $\overline{|B|^2}$ for a distributed gap with a rectangular winding. This is a constant value, independent of A. The optimal-shape winding with a single discrete gap gives lower losses than the distributed-gap design for all but very large A, corresponding to full windows that are rarely useful at high frequency anyway. Thus, by using COOS, we have not only found the best solution to accommodate the field in a gapped design, we have found a solution that is superior to the distributed-gap design that we and others have often considered ideal.

V. Application

An implementation of these designs requires a three dimensional structure, for which this two-dimensional analysis is only an approximation, albeit a much better approximation than the standard one-dimensional analysis. The construction will typically be an E- or pot-core. The gap may be placed in the center leg, in the outer legs, or both. The winding shapes developed here will have lower dc resistance when the gap is placed in the outer legs, because more of the the winding is then near the center post, where turn lengths are shorter. But a center-post gap has the advantage of low external field, particularly with a pot core. To form the winding, specially shaped bobbins and/or specially programmed automatic winding machines could be employed.

Although improved inductors could be developed for particular applications based on the techniques reported here,

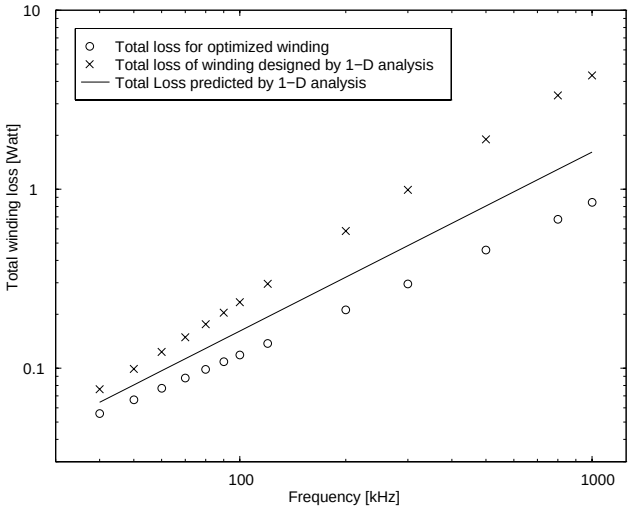

Fig. 7. Total winding loss for three different configurations. The solid line shows loss for designs optimized using one-dimensional analysis. This would be the actual loss in an optimized distributed-gap design. However, if these same designs are constructed with a lumped gap, the loss (computed by using FEA to find $\overline{|B|^2}$) will be higher, as indicated by the 'x' marks on this plot. For this, we assume the winding is spaced 2 mm from a 1-mm-long gap. The circles indicate loss with designs optimized by COOS.

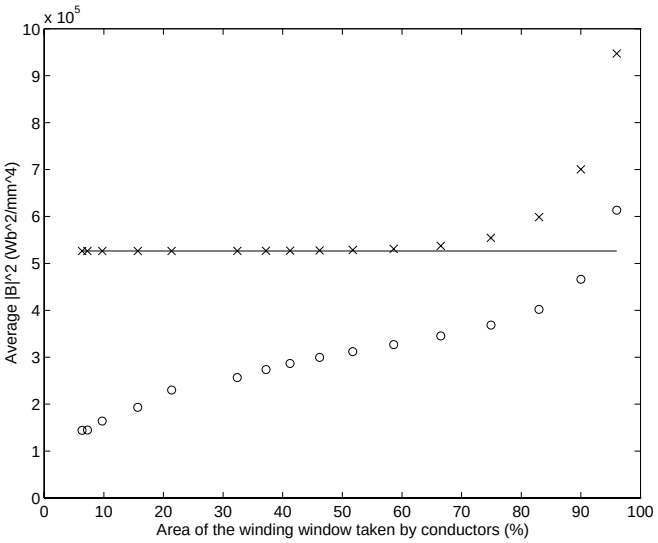

Fig. 8. Average square of magnetic field, $\overline{|B|^2}$, as a function of winding area for configurations based on three different design approaches. The proximity-effect loss is determined by $\overline{|B|^2}$, whereas the dc loss is determined by the winding area. Thus, this illustrates the design tradeoffs possible with each approach. The solid line is a rectangular winding with a distributed gap. The 'x's are designs using a rectangular winding and a lumped gap, with the winding spaced as far from the gap as possible. The circles are the optimal designs computed by COOS.

further research will be needed to fully exploit the advantages of this winding-shape optimization approach. Promising directions include remove the arbitrary fixing of litz-strand diameter, rigorously extending the analysis to three-dimensional or axially symmetric (e.g., pot core) structures, analyzing common commercial core sizes, and designing core geometries to maximize the gains made possible by optimal winding shapes.

VI. Conclusion

Through the use of specialized computational tools, we have analyzed winding shapes for gapped inductors. The results give winding configurations that not only achieve lower losses than other discretely gapped designs, but also provide lower losses than distributed-gap designs.

References

[1] A. M. Urling, A. V. Niemela, G. R. Skutt, and T. G. Wilson, "Characterizing High-Frequency Effects in Transformer Windings--A Guide to Several Significant Articles," in *APEC 89*, March 1989.

[2] P. L. Dowell, "Effects of Eddy Currents in Transformer Windings," *Proceedings of the IEE*, vol. 113, pp. 1387-1394, August 1966.

[3] J. Jongsma, "Minimum-Loss Transformer Windings for Ultrasonic Frequencies, Part 1: Background and Theory," *Phillips Electronics Applications Bulletin*, vol. E.A.B. 35, pp. 146-163, 1978.

[4] J. Jongsma, "Minimum-Loss Transformer Windings for Ultrasonic Frequencies, Part 2: Transformer winding design," *Phillips Electronics Applications Bulletin*, vol. E.A.B. 35, pp. 211-226, 1978.

[5] J. Jongsma, "High-Frequency Ferrite Power Transformer and Choke Design, Part 3: Transformer Winding Design," Phillips Electronic Components and Materials Technical Publication 207 1986.

[6] P. S. Venkatraman, "Winding Eddy Current Losses in Switch Mode Power Transformers Due to Rectangular Wave Currents," in *Proceedings of Powercon 11*, 1984.

[7] N. R. Coonrod, "Transformer Computer Design Aid for Higher Frequency Switching Power Supplies," in *IEEE Power Electronics Specialists Conference Record*, 1984.

[8] J. P. Vandelac and P. Ziogas, "A Novel Approach for Minimizing High Frequency Transformer Copper Losses," in *IEEE Power Electronics Specialists Conference Record*, 1987.

[9] J. A. Ferreira, "Improved analytical modeling of conductive losses in magnetic components.," *IEEE Transactions on Power Electronics*, vol. 9, pp. 127-31, January 1994.

[10] J. A. Ferreira, *Electromagnetic Modelling of Power Electronic Converters*: Kluwer Academic Publishers, 1989.

[11] R. Severns, "Additional losses in high frequency magnetics due to non ideal field distributions," in *APEC '92. Seventh Annual Applied Power Electronics Conference and Exposition*, Boston, MA, February 1992.

[12] D. T. N. Khai and M. H. Kuo, "Effects of Air Gaps on Winding Loss in High-Frequency Planar Magnetics," in *19th Annual Power Electronics Specialists Conf.*, April 1988.

[13] W. M. Chew and P. D. Evans, "High Frequency Inductor Design Concepts," in *22nd Annual Power Electronics Specialists Conf.*, June 1991.

[14] U. Kirchenberger, M. Marx, and D. Schroder, "A Contribution to the Design Optimization of Resonant Inductors in High Power Resonant Converters," in *1992 IEEE Industry Applications Society Annual Meeting*, October 1992.

[15] W. A. Roshen, R. L. Steigerwald, R. J. Charles, W. G. Earls, G. S. Claydon, and C. F. Saj, "High-efficiency, high-density MHz magnetic components for low profile converters," *IEEE Transaction on Industrial Applications*, vol. 31, July/August 1995.

[16] C. R. Sullivan and S. R. Sanders, "Design of Microfabricated Transformers and Inductors for High-Frequency Power Conversion," *IEEE Trans. on Power Electronics*, vol. 11, pp. 228-238, 1996.

[17] N. H. Kutkut, D. W. Novotny, D. M. Divan, and E. Yeow, "Analysis of Winding Losses in High Frequency Foil Wound Inductors," in *1995 IEEE Industry Applications Conference 30th IAS Annual Meeting*, October 1995.

[18] N. H. Kutkut and D. M. Divan, "Optimal air gap design in high frequency foil windings," in *IEEE Applied Power Electronic Conference*, Atlanta, February 1997.

[19] N. H. Kutkut, "A simple technique to evaluate winding losses including two dimensional edge effects," in *IEEE Applied Power Electronics Conference*, Atlanta, February 1997.

[20] J. Hu and C. R. Sullivan, "The quasi-distributed gap technique for planar inductors: Design guidelines," in *32nd IAS Annual Meeting*, New Orleans, October 1997.

[21] L. Ye, G. R. Skutt, R. Wolf, and F. C. Lee, "Improved winding design for planar inductors," in *28th Annual IEEE Power Electronics Specialists Conference*, St. Louis, 1997.

[22] A. J. Sinclair and J. A. Ferreira, "Optimum shape for AC foil conductors," in *Power Electronics Specialists Conference*, Atlanta, June 1995.

[23] E. C. Snelling, *Soft Ferrites, Properties and Applications, second edition*: Butterworths, 1988.

[24] C. R. Sullivan, "Optimal Choice for Number of Strands in a Litz-Wire Transformer Winding," in *28th IEEE Power Electronics Specialists Conference*, St. Louis, June 1997.

[25] J. Hu, *Design Techniques for High-Frequency Inductors—the Optimal Shape of the Winding and the Design of Quasi-Distributed Gaps*, M. S. Thesis, Thayer School of Engineering, Dartmouth College, 1998.

APPENDIX: NUMERICAL FIELD CALCULATIONS

To calculate the field in the window of a structure such as that shown in Fig. 2, we first replace the gap with an equivalent winding in an ungapped core, and then use the method of images to reduce the problem to a set of currents in a region of uniform permeability. This allows direct calculation of the field using the Biot-Savart law. These steps are described briefly below and in more detail in [25].

The process of replacing a winding with an equivalent gap can be demonstrated by magnetic circuit analysis. Fig. A1 shows an inductor structure and a corresponding magnetic circuit. The leakage reluctance, $\Re_L$, represents all the flux paths through the air other than those directly within the gap, including the gap fringing effects. The magnetic material is assumed to have infinite permeability, and so paths within it have zero reluctance. In the magnetic circuit, we can replace any reluctance with an MMF source having exactly the same MMF as appears across the original reluctance. Thus, if we replace the gap reluctance, $\Re_G$, with an MMF source of *NI*, the flux through the leakage reluctance will remain unchanged. In terms of the physical model, the gap can be replaced by a ribbon of conductor around a closed core, as shown in Fig. A2, with current *NI*, oriented to oppose the winding current. The equivalence can be demonstrated by other analytical approaches and verified by finite-element analysis [25]. For a two-dimensional model, only the strip of current inside the window is needed for calculations of the field inside the window.

Given the two dimensional model with a closed core, the winding, and an opposing "gap current", we can approach the calculation of the field using the method of images—each flat side of the window, of infinite permeability material can be removed from the model if image currents corresponding to those in the original window are placed appropriately. Like a room lined with mirrors, the winding window surrounded by a closed core implies an infinite number of images for each original current filament. Fortunately, the net field from any given image window drops off rapidly with distance, because the winding and gap currents are equal and opposite. The original window is first grouped with an image on the gap side, to form a symmetric pair. This pair is then reproduced in a grid of further images. A 3 x 3 grid of these pairs gives about 1% error in the field, while a 5 x 5 grid gives less than 0.01% error. We used at least a 5 x 5 grid for the results presented here. Given this grid of image currents, the field at any given point in the original window can be calculated by simply summing the field component due to each current element.

For the purpose of optimizing winding shape, the field calculations as outlined above are performed individually for individual current filaments at each position in a grid of within the window. These calculations are then stored and can be combined by superposition to calculate the field with any given combination of current filaments representing a winding shape.

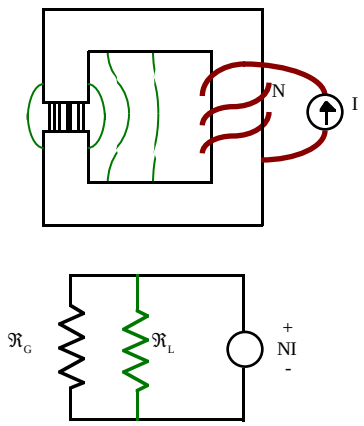

Fig. A1. Gapped inductor and corresponding magnetic circuit

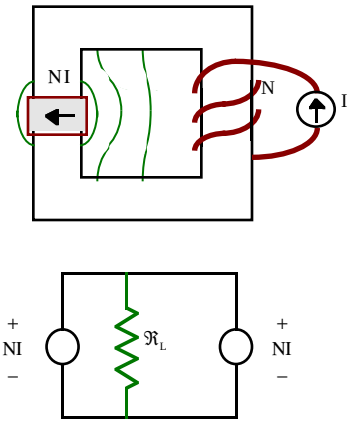

Fig. A2. Equivalent structure and corresponding magnetic circuit.

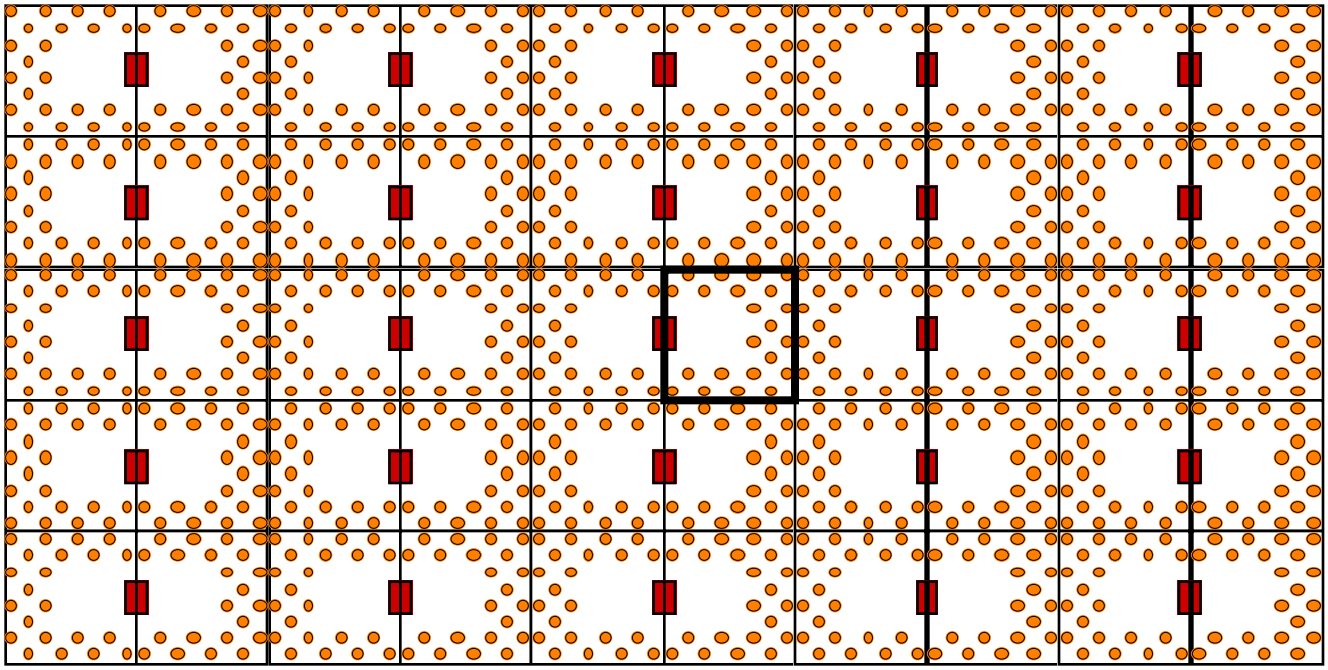

Fig. A3. Array of image currents used to calculate the field in the winding window. The original winding window near the center is outlined with a dark square, and includes round wire windings and a current representing the gap. This original with its image to the left are repeated in a 5 x 5 array of images.